

---

## EVALUATION OF CATALYTIC IMPLEMENTATION OF SPINEL $\text{CoFe}_2\text{O}_4$ -LOADED NaY IN DIRECT HYDROXYLATION OF BENZENE TO PHENOL

---

Mohamed S. Thabet<sup>1,2</sup>, Adham A. El-Zomrawy<sup>1\*</sup>

<sup>1</sup>*Department of Chemistry, Faculty of Science, Al-Azhar University, Nasr City 11884, Cairo, Egypt*

<sup>2</sup>*Department of Chemistry, Faculty of Science, Jazan University, Saudi Arabia*

\*Correspondence to email: azomrawy@yahoo.com

---

### ABSTRACT

Spinel cobalt ferrite  $\text{CoFe}_2\text{O}_4$  was synthesized and in situ incorporated onto the porous structure of NaY zeolite by the co-precipitation process. The structural design of  $\text{CoFe}_2\text{O}_4/\text{NaY}$  composite was advantageous in terms of activity and stability. Various techniques were utilized to characterize the catalysts like X-ray diffraction (XRD), Fourier transform infrared spectroscopy (FTIR), scanning electron microscopy (SEM) and pore structure analysis by  $\text{N}_2$  adsorption at 77 K. It has been found that spinel  $\text{CoFe}_2\text{O}_4$  in  $\text{CoFe}_2\text{O}_4/\text{NaY}$  was sparse on the NaY surface, along with the relevant species inside the zeolite pores. The SEM surface morphology suggests that  $\text{CoFe}_2\text{O}_4$  has an irregular structure of large aggregated crystals, whereas  $\text{CoFe}_2\text{O}_4/\text{NaY}$  exhibited predominantly a uniform spherical-like morphology of smaller particle sizes and small cavities on the external surface. The direct hydroxylation of benzene with  $\text{H}_2\text{O}_2$  as a green oxidant was inspected. The effects of the amount of test dose of the  $\text{CoFe}_2\text{O}_4/\text{NaY}$  catalyst, concentration of  $\text{H}_2\text{O}_2$ , and the reaction temperature were studied. Higher yield of phenol was obtained with increasing the concentration of  $\text{H}_2\text{O}_2$ , catalyst dose and temperature. The kinetics of the hydroxylation of benzene to phenol has shown that the catalyst dose was highly affected reaction rate. The Arrhenius relationship was applied to determine the activation energy of the reaction to be 25.98 kJ/Mol.

**Keywords:** hydroxylation; benzene; phenol; composite; kinetics.

### 1. INTRODUCTION

Phenol is an industrial commodity as a precursor to many remarkable materials such as phenolic resins epoxied, pharmaceutical drugs, plastic, and detergents [1]. The fumes process for preparation of phenol is cumene; the disadvantages of commercial process were due to complex of phenolic derivatives, difficult separation of products and extreme complicated trouble in an organic synthesis field from economic and environmental point of view [2-4]. In the search to minimize these disadvantages, the heterogenization of homogeneous catalysts has emerged as a focus of research. A heterogeneous catalysis process is easily reusable and recoverable when compared with the homogeneous ones. Zeolites are openly used in several implementations, from heterogeneous catalysis to environment friendly [5]. Zeolites or modified zeolite, transition metals, polyoxometalate and ferrites have been extremely studied in heterogeneous

catalysis for hydroxylation of benzene to phenol [6,7].

Spinel transition metal ferrites [ $\text{M}^{2+}(\text{Fe}_2\text{O}_4)$ ],  $\text{M} = \text{Mg}, \text{Cr}, \text{Co}, \text{Mn}, \text{Ni}, \text{Zn}$ , etc., are potentially valuable in a broad range of applications due to their high stability, low-cost, environmentally friendly and high catalytic activity [8-11]. Spinel ferrites can be classified into different types based on the composition and distribution of cations. Among spinel ferrites,  $\text{CoFe}_2\text{O}_4$  has been considered as one of the most important materials for its good structural stability as well as notable physical and chemical properties. The  $\text{CoFe}_2\text{O}_4$  compound is a well-known spinel including  $\text{Co}^{2+}$  and  $\text{Fe}^{3+}$  ions distributed between the octahedral and tetrahedral sites, respectively. Works of many researchers had assumed that spinel  $\text{CoFe}_2\text{O}_4$  has ions at different geometrical sites that could be effectively play a crucial role in tuning the properties of ferrite particles for various technological applications.

Preparation methods of ferrite samples play a decisive role in the consequence of the physicochemical properties of ferrite particles [12-15]. Such preparation methods should have a control over the desired stoichiometric ratio, particle size, morphology etc. [16,17].

There are many techniques like hydrothermal process, thermolysis, co-precipitation, gel-assisted hydrothermal process, for the preparation of  $\text{CoFe}_2\text{O}_4$ . A co-precipitation method is particularly efficient that provides a very simple preparation procedure and has good control over particle size and composition [18-22].

In this work, we have prepared a novel hybrid composite comprised of  $\text{CoFe}_2\text{O}_4$  spinel oxide loaded onto NaY zeolite ( $\text{CoFe}_2\text{O}_4/\text{NaY}$ ), by the co-precipitation method.  $\text{CoFe}_2\text{O}_4$  spinel oxide exhibits excellent bifunctional catalytic properties towards hydroxylation of benzene to phenol by  $\text{H}_2\text{O}_2$ . The modified catalyst ( $\text{CoFe}_2\text{O}_4/\text{NaY}$ ) could display two main advantages in this reaction. (1) The contact time between the reactants and the  $\text{CoFe}_2\text{O}_4/\text{NaY}$  catalyst expands because of permitting a high surface area. (2) The catalyst can easily be separated from the admixture of reaction by applying an exterior magnet. The ability to direct transformation of benzene to phenol is a likable and would be viewed by a lot of investigators [23-28]. Hydrogen peroxide is a highly green oxidant due to by-products are environmentally friendly as studied by many researchers [29-31]. The liquid conversion with hydrogen peroxide on the  $\text{CoFe}_2\text{O}_4/\text{NaY}$  catalyst at different conditions was investigated.

## 2. EXPERIMENTAL

### 2.1. Materials

Cobalt nitrate (Merck), ferric nitrate (Merck), ammonium hydroxide (28%, Merck), benzene (99%, Merck), 4-aminoantipyrine (98%, Sigma-Aldrich),  $\text{H}_2\text{O}_2$  (30%, Qualigens) and NaY zeolite (Himedia Laboratories Pvt.Ltd) were used in the experiments.

### 2.2. Preparation of $\text{CoFe}_2\text{O}_4$

Fine particles of  $\text{CoFe}_2\text{O}_4$  were prepared using the co-precipitation method. A mixed aqueous solution of cobalt nitrate and ferric nitrate with a molar ratio of 1/2 was freshly

prepared and heated to 343 K. The solution pH was adjusted to 7 while stirring by adding drops of ammonium hydroxide solution. These Co/Fe molar ratio and solution pH were found crucial to obtain stoichiometric  $\text{CoFe}_2\text{O}_4$ . To ensure complete growth of the crystals, the reaction was kept at 343 K for 2 h. After turning off the stirrer, the settled down crystals were collected via discarding the top water layer. The washed crystals with distilled water to remove unwanted ions were then dried at 373 K for 5 h, then calcined at 623 K for 3 h and this sample was referred to as  $\text{CoFe}_2\text{O}_4$ .

### 2.2.1. *In situ* preparation of $\text{CoFe}_2\text{O}_4/\text{NaY}$ composite

$\text{CoFe}_2\text{O}_4$  sample was *in situ* prepared in the presence of NaY zeolite by the co-precipitation method according to Huang et.al.[32]. Certain amounts of ferric nitrate and cobalt nitrate each dissolved in distilled water was added to 10 g NaY zeolite and stirred for 15 min at room temperature. The metal solution of desired concentration was adapted at Co/Fe molar ratio of 1/2 to obtain the target sample. The pH was adjusted at about 10 by adding ammonium hydroxide solution drop wise to complete the co-precipitation of the precursor ferrite in the manifestation of NaY zeolite. The mixture was then filtered and washed to neutral pH. The solid precipitate thus obtained was dried in an oven at 393 K for 1 h, and then calcined at 623 K for 3 h.

### 2.3. Physicochemical characterization

The final prepared  $\text{CoFe}_2\text{O}_4$  and  $\text{CoFe}_2\text{O}_4/\text{NaY}$  samples were characterized by XRD using a *PANalytical*, PRO diffractometer. The patterns were run with  $\text{CuK}_\alpha$  radiation wavelength ( $\lambda = 1.54056$ ) and scanning speed of  $2\theta = 2.5^\circ/\text{min}$ .

FTIR spectra were recorded on a FT/IR-4100 spectrophotometer type A, serial number (C204261016) and a spectral resolution of  $4 \text{ cm}^{-1}$  within the range from  $350-4000 \text{ cm}^{-1}$ .

Morphology test was determined using a JEOL JSM-5500 Scanning Electron Microscope (SEM) at an accelerating voltage of 25 KV.

The amount of phenol produced was determined by a Shimadzu spectrophotometer (UV\*1800, ENG 240V, soft Japan) according

to the 4-aminoantipyrine spectroscopic method of phenol analysis.

The surface textures, the pore volume and pore distribution were studied using the BET and BJH method at 77 K using Quantachrome Nova Win instrument version 11.04.

#### 2.4. Catalytic reaction

Liquid-phase hydroxylation of benzene to phenol was performed in a three necked round flask (250 ml) with reflux under appropriate temperature (333-353 K) and atmospheric pressure with continuous stirring. In the model experiment, 0.05-0.15 g of catalyst was suspended in 50 ml of pure benzene, after fixing at the appropriate temperature reaction, H<sub>2</sub>O<sub>2</sub> (30%) (0.033- 0.229 mol) was added drop wise within 30 min. The reaction was executed for 3 h at 343 K with stirring. After the reaction has been stopped, the concentration of phenol being obtained solely was determined at  $\lambda_{\text{max}} = 510$  nm using spectrophotometer by the 4-aminoantipyrine method.

### 3. RESULT AND DISCUSSION

#### 3.1. Phase analysis by XRD

X-ray diffraction (XRD) analysis was carried out to assess the phase composition of the different samples. XRD pattern of NaY, CoFe<sub>2</sub>O<sub>4</sub> and CoFe<sub>2</sub>O<sub>4</sub>/NaY composite are shown in Fig. 1. The CoFe<sub>2</sub>O<sub>4</sub> sample shows sharp bands at  $2\theta$  of 24.3°, 26°, 28.9°, 33.5°, 36°, 37.8°, 41.3°, 50°, 55°, 57.5°, 63.3°, 66°, and 73° which indicate the occurrence of successfully prepared cubic spinel particles of CoFe<sub>2</sub>O<sub>4</sub> [33]. Meanwhile, the XRD pattern of the CoFe<sub>2</sub>O<sub>4</sub>/NaY composite displays an ultimately identical pattern to that of the bare NaY zeolite. The intensities of the peaks in the composite sample decreased as compared with those of the parent zeolite sample. Besides, shift of XRD peaks characteristic of NaY zeolite after modification with CoFe<sub>2</sub>O<sub>4</sub> was observed. These reflection changes seem to involve the incorporation and dispersion of the spinel ferrite species in the zeolite framework structure. The crystal size of samples identified using the Scherrer equation are 34 and 31 nm for parent and composite, respectively.

Scanning electron microscopy (SEM) images of the parent NaY zeolite and CoFe<sub>2</sub>O<sub>4</sub>/NaY composite are presented in Fig.

2. The surface morphology via the SEM image in Fig. 2a suggests that CoFe<sub>2</sub>O<sub>4</sub> has an irregular structure of large aggregated crystals, whereas images of CoFe<sub>2</sub>O<sub>4</sub> (Fig. 2b) and parent NaY (Fig. 2c) exhibit predominantly a uniform spherical-like morphology of smaller particle sizes with small cavities on the external surface. The lowering of particle size of CoFe<sub>2</sub>O<sub>4</sub>/NaY compared with that of neat CoFe<sub>2</sub>O<sub>4</sub> implies interaction between CoFe<sub>2</sub>O<sub>4</sub> and the NaY surfaces.

FTIR spectra of the NaY, CoFe<sub>2</sub>O<sub>4</sub> and CoFe<sub>2</sub>O<sub>4</sub>/NaY catalysts in the 4000-350 cm<sup>-1</sup> region are shown in Fig.3. The characteristic spectral region of CoFe<sub>2</sub>O<sub>4</sub> is the absorption in the area between 400-600 cm<sup>-1</sup> [34,35]. This region points to spinel structure phase, where Co<sup>+2</sup> and Fe<sup>+3</sup> ions occupy the octahedral and tetrahedral sites, respectively. The band at 580 cm<sup>-1</sup> was assigned to the Fe-O group [36,37], but no vibrations of the Co-O linkage could be detected. The FTIR spectrum of the NaY zeolite shows bands around 1001, 970, 662, 552, 461 and 390 cm<sup>-1</sup> attributed to the zeolite framework according to references [30, 38-39]. The main distinguish region in the spectral between 400 and 1200 cm<sup>-1</sup> resulted from stretching and bending vibration of the T-O units in zeolite structure. The band at 566 cm<sup>-1</sup> is characteristic of the faujasite NaY zeolite [40]. The spectrum of CoFe<sub>2</sub>O<sub>4</sub>/NaY reveals all the bands related to zeolite structure. The absorptions related to the spinel CoFe<sub>2</sub>O<sub>4</sub> structure was not appeared plausibly due to peaks overlapping resulting from spectral features of the CoFe<sub>2</sub>O<sub>4</sub> and NaY zeolite and/or lower concentration of the former in the composite sample [41].

The adsorption-desorption isotherms were measured at 77 K for the parent NaY zeolite and CoFe<sub>2</sub>O<sub>4</sub>/NaY sample as shown in Fig. 4. The specific surface area was obtained by the BET method, but the pore volume and pore-size distribution were calculated using the BJH method. The isotherm of the NaY zeolite is likely belong to type I as defined by IUPAC, which is characteristic of microporous materials. The start of hysteresis loop at  $p/p^{\circ} \approx 0.65$  seen in the isotherm of CoFe<sub>2</sub>O<sub>4</sub>/NaY suggests switching to type IV that arises from the N<sub>2</sub> condensation in the mesopores of the sample. This may be due to the presence of

CoFe<sub>2</sub>O<sub>4</sub> species in the pores of NaY zeolite as confirmed by the XRD and SEM analyses. The non-saturation at P/P° = 0.9 shown in the isotherm of CoFe<sub>2</sub>O<sub>4</sub>/NaY may be attributed to the distance between interacting CoFe<sub>2</sub>O<sub>4</sub> moieties with the zeolite framework.

Figure 5 shows the pore size distribution of NaY sample which displayed a pore covering in the range between 18 to 34 Å with a maximum at 18 Å, whereas that of the CoFe<sub>2</sub>O<sub>4</sub>/NaY composite shows a bimodal distribution at 16 to 50 Å, indicating an increase in the mesoporosity of this sample. The data of surface texture of samples are listed in Table 1. The relative decrease in the surface area of CoFe<sub>2</sub>O<sub>4</sub>/NaY compared to that of NaY signifies the penetration of CoFe<sub>2</sub>O<sub>4</sub> species inside the pores of zeolite. Meanwhile, there is a concurrent increase in the total pore volume of CoFe<sub>2</sub>O<sub>4</sub>/NaY as compared with that of NaY, a good suggestion of the presence of CoFe<sub>2</sub>O<sub>4</sub> aggregates on the external surface coexisting with dispersed ones inside the pores of zeolite. The clear increase in the average pore radius ( $\bar{r}$ ) of the CoFe<sub>2</sub>O<sub>4</sub>/NaY sample compared with that of parent NaY zeolite (Table 1) reflects the widening of zeolite pores as a result of the implement location of CoFe<sub>2</sub>O<sub>4</sub> onto the pores of zeolite.

### 3.2. Oxidation of benzene to phenol

Hydroxylation of benzene to phenol with H<sub>2</sub>O<sub>2</sub> as an oxidant has been studied using CoFe<sub>2</sub>O<sub>4</sub>/NaY composite as the catalyst. The parameters selected for analysis were the concentration of H<sub>2</sub>O<sub>2</sub>, reaction temperature, and amount of catalyst.

#### 3.2.1. Effect of H<sub>2</sub>O<sub>2</sub> concentration

The effect of the amount of H<sub>2</sub>O<sub>2</sub> on the hydroxylation of benzene to phenol has been investigated with 0.1 g of CoFe<sub>2</sub>O<sub>4</sub>/NaY catalyst at 333 K. The effect of H<sub>2</sub>O<sub>2</sub> on the produce phenol was represented in Fig. 6a. The amount of phenol produced increases steadily using increasing concentrations of hydrogen peroxide from 0.033 to 0.229 mol. The yield of phenol reached a maximum (8.51 %) at 7.0 mL H<sub>2</sub>O<sub>2</sub> (0.229 mol) (Fig. 7).

#### 3.3. Effect of catalyst dose

Direct hydroxylation of benzene to phenol by using various doses of the CoFe<sub>2</sub>O<sub>4</sub>/NaY catalyst was further investigated with 0.136 mol of hydrogen peroxide at 333 K. The yield of phenol versus the dose of catalyst is shown in Fig. 7. It was observed that the increase of the CoFe<sub>2</sub>O<sub>4</sub>/NaY mass from 0.05 to 0.15 g had led to increase the number of moles of phenol produced over time (Fig. 6b). This denotes the dependence of the reaction rate on the catalyst dose [42,43].

#### 3.4. Effect of reaction temperature

To investigate the effect of temperature on the conversion of benzene to phenol, the temperature varied from 333 to 353K (Fig. 7), with the other parameters being kept constant (i.e. 0.163 mole of H<sub>2</sub>O<sub>2</sub> and 0.1 g of the CoFe<sub>2</sub>O<sub>4</sub>/NaY composite), and over a variable time period at a fixed temperature (Fig. 6c). The yield of produced phenol increases with increasing reaction temperature from 7.1 to 13.67 % (Figs. 6c and 7).

In general, Fig. 7 represent the lower yield of phenol production, it was attributed to the

**Table 1.** Surface texture and pore structure of the samples calculated from N<sub>2</sub> adsorption- desorption isotherms using the spectrometry method.

parameters	NaY	composite
surface area, m <sup>2</sup> /g	191.40	180.82
adsorption cumulative surface area, m <sup>2</sup> /g	126.00	167.90
external surface area, m <sup>2</sup> /g	128.50	180.20
micropore surface area, m <sup>2</sup> /g	62.82	----
Total pore volume	0.05261	0.0772
adsorption cumulative pore volume, cm <sup>3</sup> /g	0.191	0.353
C constant	2.713	10.825
Average pore radius	5.499	8.570
adsorption pore radius, $\bar{r}$ (Å)	15.22	18.63

self-degradation of hydrogen peroxide of higher temperatures.

### 3.5. Kinetic studies

Different variables of kinetic studies for the hydroxylation of benzene to phenol can be examined. Among important variables, the amount of hydrogen peroxide,  $\text{CoFe}_2\text{O}_4/\text{NaY}$  catalyst and temperature. Reaction-rate data were summarized by the following equation based upon a first order:

$$\ln(C_o - C_t) = -kt + \ln C_o \quad (1)$$

where  $C_o$  is the initial concentration,  $C_t$  is the variation of concentration against time ( $t$ ), and  $k$  is the rate constant. The experimental data were fitted with Eq. (1), and the basic parameters were listed in Table 2. The kinetics of the hydroxylation of benzene with 0.1 g of  $\text{CoFe}_2\text{O}_4/\text{NaY}$  catalyst at 333 K were studied in the presence of different amounts of hydrogen peroxide. The impact of the number of moles of  $\text{H}_2\text{O}_2$  on the rate of reaction is shown in Fig. 8. It is obvious that the rate of the reaction increases progressively with increasing initial concentration of  $\text{H}_2\text{O}_2$  up to 0.229 mol. Moreover, the  $\text{CoFe}_2\text{O}_4/\text{NaY}$  dosage was highly affected on the reaction rate in the presence of 0.163 mol hydrogen peroxide at 333 K. Also, the efficiency of the reaction was

tested at the range 333 to 353 K in the presence of 0.1 g of  $\text{CoFe}_2\text{O}_4/\text{NaY}$  and 0.163 mol  $\text{H}_2\text{O}_2$ . The rate constant of the reaction was found to increase by increasing the reaction temperature up to 353 K.

The amount of benzene in the reaction was 11.2 mol, while the highest concentration of hydrogen peroxide was 0.229 mol. Consequently, the concentration of benzene was much higher, so the reaction was dependent on  $\text{H}_2\text{O}_2$  only.

### 3.6. Activation energy

The values of the rate constant,  $k$ , increased with increase the temperature from 333 to 353 K. The Arrhenius expression for the temperature dependence of the rate is applied, as shown by Eq. (2),

$$\ln k = -E_a / RT + \ln A \quad (2)$$

where  $E_a$ ,  $R$  and  $T$  are the Arrhenius activation energy, the gas constant, and the absolute temperature, respectively.

A relation between  $\ln k$  versus the inverse of the temperature is stated in Fig. 9. A linear relationship between the rate constant and temperature was obtained with correlation coefficient ( $R^2$ ) of 0.9490, and the activation energy for this reaction was  $\approx 25.98$  kJ/mol.

**Table 2:** Different variables of kinetic parameters for the catalytic hydroxylation of benzene to phenol.

	$C_o$ (Exp.) (mol)	$C_o$ (Calc.) (mol)	$k$ ( $\text{hr}^{-1}$ )	$t_{1/2}$ (hr)	$r^2$
$\text{H}_2\text{O}_2$ (mol)	0.033	11.192	0.004	172.8	0.9815
	0.065	11.182	0.013	53.5	0.9770
	0.131	11.182	0.020	34.1	0.9902
	0.163	11.171	0.027	26.0	0.9935
	0.229	11.177	0.035	19.7	0.9981
$\text{CoFe}_2\text{O}_4/\text{NaY}$ (g)	0.05	11.186	0.022	31.5	0.9927
	0.10	11.221	0.027	26.0	0.9935
	0.15	11.154	0.032	21.6	0.9936
Temp. (K)	333	11.171	0.027	26.0	0.9935
	338	11.172	0.033	20.8	0.9908
	343	11.154	0.038	18.1	0.9818
	348	11.147	0.044	15.9	0.9817
	353	11.141	0.045	15.3	0.9894

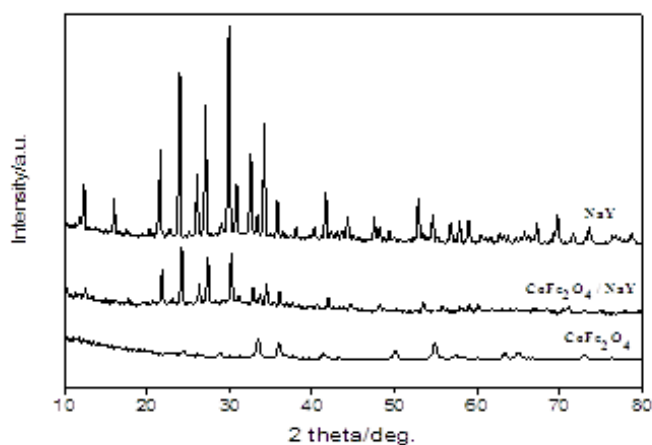


**Fig. 1:** X-ray powder diffraction patterns of NaY, CoFe<sub>2</sub>O<sub>4</sub>/NaY and CoFe<sub>2</sub>O<sub>4</sub>.

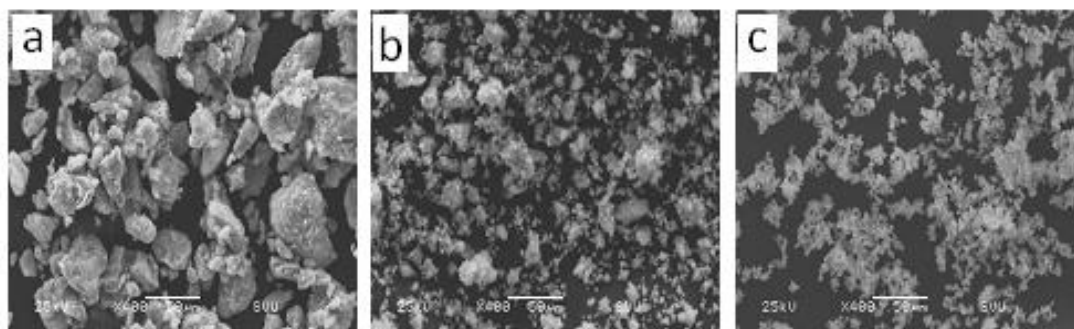


**Fig. 2:** SEM images of a) CoFe<sub>2</sub>O<sub>4</sub>, b) CoFe<sub>2</sub>O<sub>4</sub>/NaY and c) NaY.

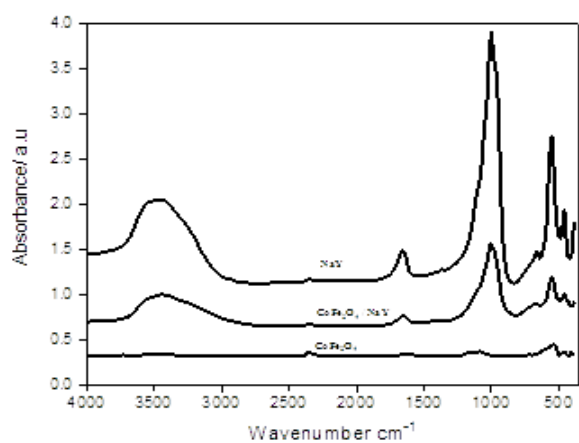


**Fig. 3:** FTIR spectra of NaY, CoFe<sub>2</sub>O<sub>4</sub>/NaY and CoFe<sub>2</sub>O<sub>4</sub>

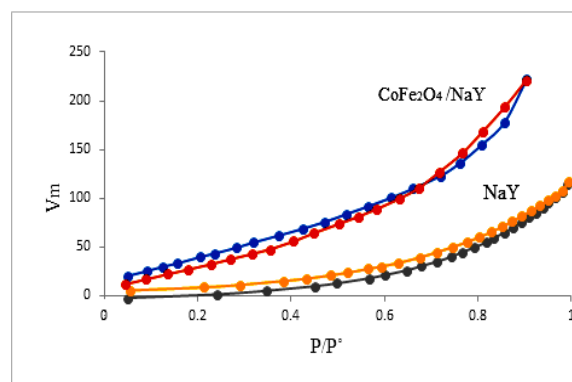


**Fig. 4:** Adsorption –desorption isotherms of N<sub>2</sub> at 77 K for NaY, CoFe<sub>2</sub>O<sub>4</sub>/NaY.

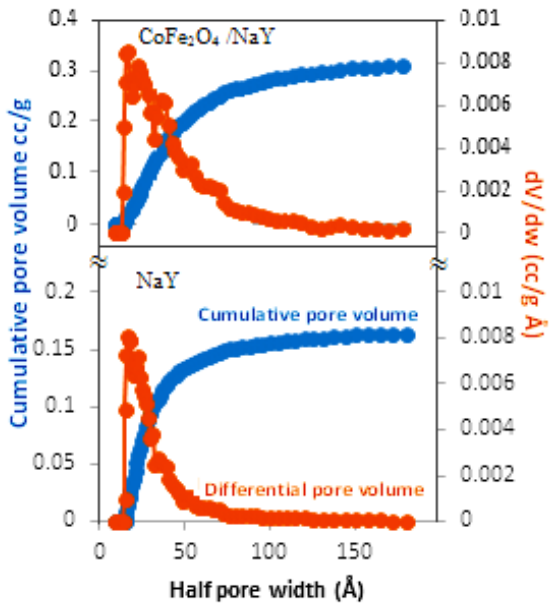


Fig. 5: Particle size distribution of NaY and CoFe<sub>2</sub>O<sub>4</sub>/NaY

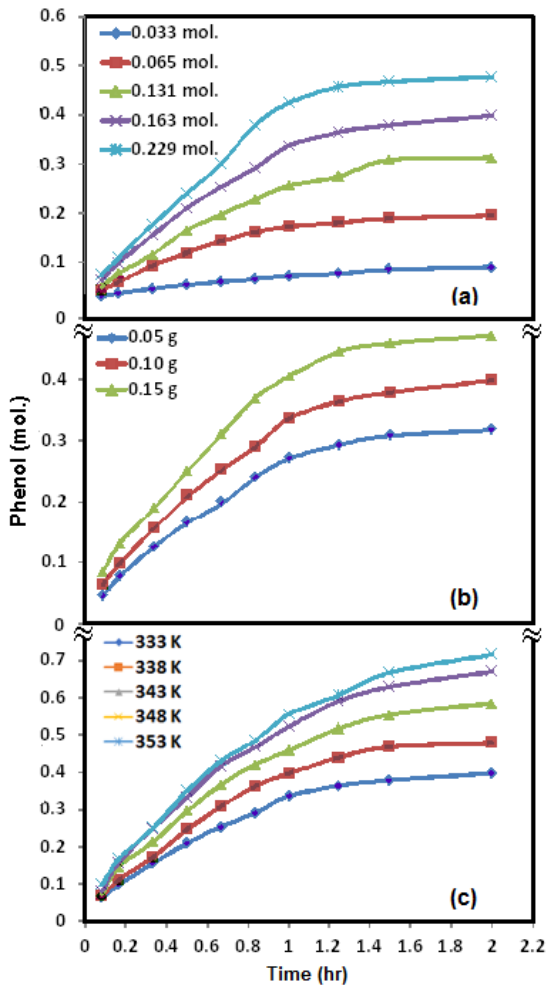


Fig. 6: Effect of (a) H<sub>2</sub>O<sub>2</sub>, (b) dose of catalyst, and (c) reaction temperature on the production yield of phenol.

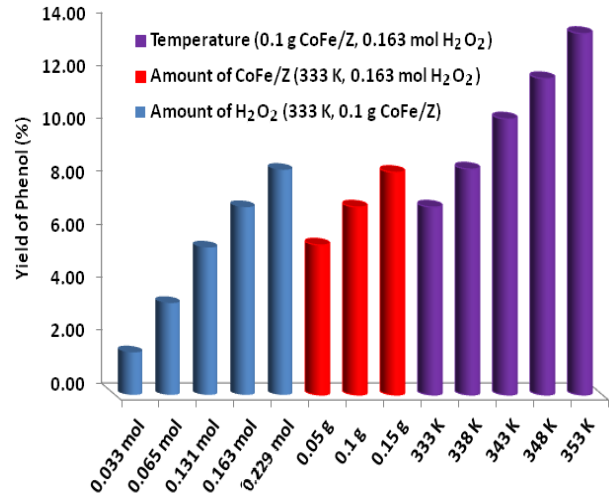


Fig. 7: Phenol yield as a function of temperature of reaction, amount of catalyst and concentration of hydrogen peroxide.

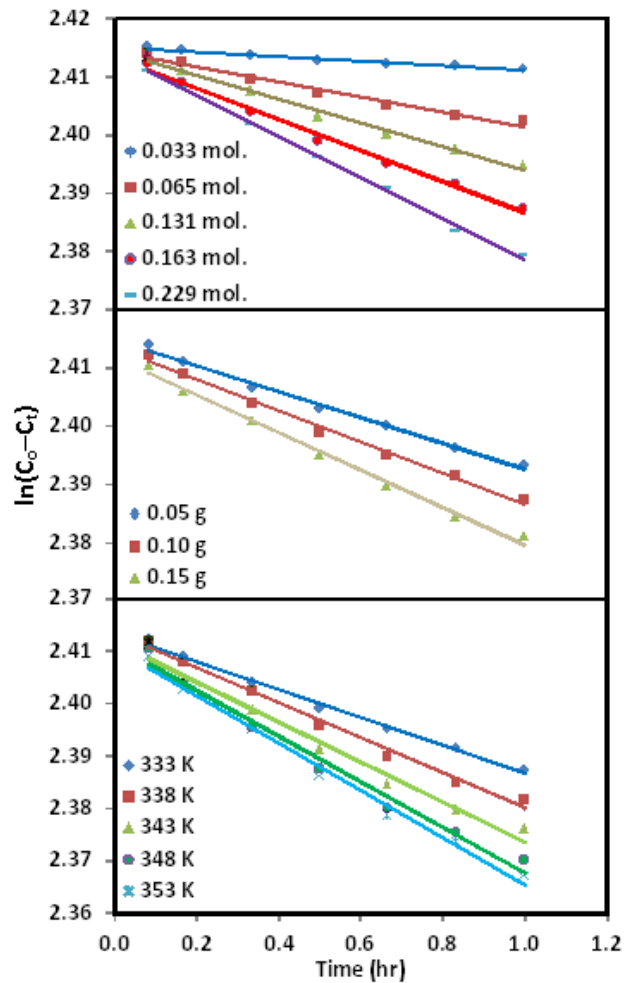


Fig. 8: The kinetics of the hydroxylation of benzene at different parameters.

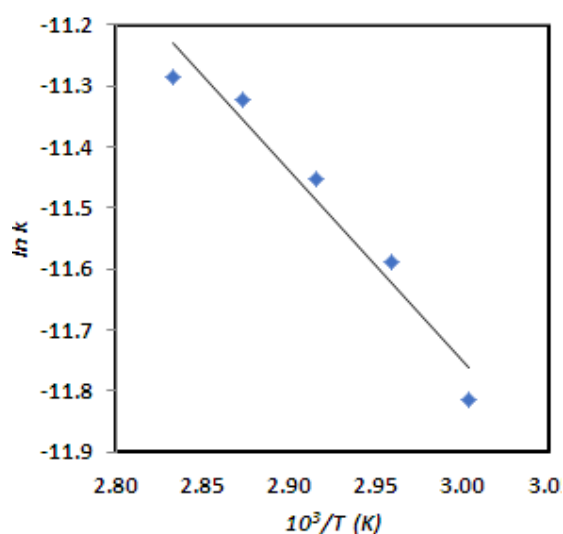


Fig. 9: The relation between  $\ln k$  versus the inverse of temperature.

#### 4. CONCLUSION

A novel composite of spinel  $\text{CoFe}_2\text{O}_4$  loaded on NaY ( $\text{CoFe}_2\text{O}_4/\text{NaY}$ ) was prepared, and it was characterized using many techniques such as XRD, FTIR, surface texture, and SEM. The catalytic effect of the  $\text{CoFe}_2\text{O}_4/\text{NaY}$  composite catalyzed direct hydroxylation of benzene to phenol in the presence of hydrogen peroxide was studied. Several parameters have been identified for promoting this reaction such as concentration of  $\text{H}_2\text{O}_2$ , temperature, and amount of catalyst. The results have been shown that the yield of phenol increased with increasing the amounts of  $\text{H}_2\text{O}_2$ , catalyst dose and temperature. This has also been evidenced from the half-life values calculated from the kinetics of the reaction.

#### REFERENCES

- [1] L. Meng, X. Zhu, and E. J. M. Hensen, "Stable Fe/ZSM-5 Nanosheet Zeolite Catalysts for the Oxidation of Benzene to Phenol," *ACS Catal.*, vol. 7, no. 4, pp. 2709–2719, Apr. 2017.
- [2] K. Weissmehl, H.-J. Arpe, C. R. Lindley, and S. Hawkins, *Industrial organic chemistry*, vol. 2. Wiley Online Library, 1997.
- [3] R. J. Schmidt, "Industrial catalytic processes—phenol production," *Appl. Catal. Gen.*, vol. 280, no. 1, pp. 89–103, 2005.
- [4] J. Peng, F. Shi, Y. Gu, and Y. Deng, "Highly selective and green aqueous–ionic liquid biphasic hydroxylation of benzene to phenol with hydrogen peroxide," *Green Chem.*, vol. 5, no. 2, pp. 224–226, 2003.
- [5] A. Fan, G. K. Chuah, and S. Jaenicke, "A novel and environmental friendly synthetic route for hydroxypyrrolidines using zeolites," *Carbohydr. Res.*, vol. 472, pp. 103–114, 2019.
- [6] A. E. ElMetwally, G. Eshaq, F. Z. Yehia, A. M. Al-Sabagh, and S. Kegn'a es, "Iron oxychloride as an efficient catalyst for selective hydroxylation of benzene to phenol," *Acs Catal.*, vol. 8, no. 11, pp. 10668–10675, 2018.
- [7] H. Wang, C. Wang, M. Zhao, Y. Yang, L. Fang, and Y. Wang, "H5PMo10V2O40 anchor by OH of the Titania nanotubes: Highly efficient heterogeneous catalyst for the direct hydroxylation of benzene," *Chem. Eng. Sci.*, vol. 177, pp. 399–409, 2018.
- [8] J. Chen, K. Zhao, Z. Zhao, F. He, Z. Huang, and G. Wei, "Identifying the roles of  $\text{MFe}_2\text{O}_4$  (M= Cu, Ba, Ni, and Co) in the chemical looping reforming of char, pyrolysis gas and tar resulting from biomass pyrolysis," *Int. J. Hydrog. Energy*, vol. 44, no. 10, pp. 4674–4687, 2019.
- [9] M. T. Jamil *et al.*, "Effect on structural and optical properties of Zn-substituted cobalt ferrite  $\text{CoFe}_2\text{O}_4$ ," *J. Ovonic Res.*, vol. 13, no. 1, pp. 45–53, 2017.
- [10] G. Raju *et al.*, "Effect of chromium substitution on the structural and magnetic properties of cobalt ferrite," *Mater. Sci. Energy Technol.*, vol. 2, no. 1, pp. 78–82, 2019.
- [11] O. Karaagac, B. B. Yildiz, and H. Köçkar, "The influence of synthesis parameters on one-step synthesized superparamagnetic cobalt ferrite nanoparticles with high saturation magnetization," *J. Magn. Magn. Mater.*, vol. 473, pp. 262–267, 2019.
- [12] Z. Zhu, F. Liu, H. Zhang, J. Zhang, and L. Han, "Photocatalytic degradation of 4-chlorophenol over  $\text{Ag}/\text{MFe}_2\text{O}_4$  (M= Co, Zn, Cu, and Ni) prepared by a modified chemical co-precipitation method: a comparative study," *Rsc Adv.*, vol. 5, no. 68, pp. 55499–55512, 2015.
- [13] Z. Naghshbandi, N. Arsalani, M. S. Zakerhamidi, and K. E. Geckeler, "A novel synthesis of magnetic and photoluminescent graphene quantum dots/ $\text{MFe}_2\text{O}_4$  (M= Ni, Co) nanocomposites for catalytic application," *Appl. Surf. Sci.*, vol. 443, pp. 484–491, 2018.

- [14] I. Othman, M. Abu Haija, and F. Banat, "Catalytic Properties of Phosphate-Coated  $\text{CuFe}_2\text{O}_4$  Nanoparticles for Phenol Degradation," *J. Nanomater.*, vol. 2019, 2019.
- [15] C. Si *et al.*, "Mesoporous nanostructured spinel-type  $\text{MFe}_2\text{O}_4$  (M= Co, Mn, Ni) oxides as efficient bi-functional electrocatalysts towards oxygen reduction and oxygen evolution," *Electrochimica Acta*, vol. 245, pp. 829–838, 2017.
- [16] Z. P. Niu, Y. Wang, and F. S. Li, "Magnetic properties of nanocrystalline Co–Ni ferrite," *J. Mater. Sci.*, vol. 41, no. 17, pp. 5726–5730, 2006.
- [17] P. Lavela, J. L. Tirado, and C. Vidal-Abarca, "Sol-gel preparation of cobalt manganese mixed oxides for their use as electrode materials in lithium cells," *Electrochimica Acta*, vol. 52, no. 28, pp. 7986–7995, 2007.
- [18] R. T. Olsson, G. Salazar-Alvarez, M. S. Hedenqvist, U. W. Gedde, F. Lindberg, and S. J. Savage, "Controlled synthesis of near-stoichiometric cobalt ferrite nanoparticles," *Chem. Mater.*, vol. 17, no. 20, pp. 5109–5118, 2005.
- [19] R. R. Powar, A. B. Gadkari, P. B. Piste, and D. N. Zambare, "Synthesis and characterization study of dual phase mixed zinc cobalt ferrite nanoparticles prepared via chemical co-precipitation method," 2018.
- [20] J. Thomas *et al.*, "Synthesis of cobalt ferrite nanoparticles by constant pH co-precipitation and their high catalytic activity in CO oxidation," *New J. Chem.*, vol. 41, no. 15, pp. 7356–7363, 2017.
- [21] A. Kalam *et al.*, "Modified solvothermal synthesis of cobalt ferrite ( $\text{CoFe}_2\text{O}_4$ ) magnetic nanoparticles photocatalysts for degradation of methylene blue with  $\text{H}_2\text{O}_2$ /visible light," *Results Phys.*, vol. 8, pp. 1046–1053, 2018.
- [22] S. Sinhamahapatra, M. Shamim, H. S. Tripathi, A. Ghosh, and K. Dana, "Kinetic modelling of solid state magnesium aluminate spinel formation and its validation," *Ceram. Int.*, vol. 42, no. 7, pp. 9204–9213, 2016.
- [23] P. Xiao, Y. Wang, J. N. Kondo, and T. Yokoi, "Consequences of Fe speciation in MFI zeolites for hydroxylation of benzene to phenol with  $\text{H}_2\text{O}_2$ ," *Appl. Catal. Gen.*, vol. 579, pp. 159–167, 2019.
- [24] Y. Luo, J. Xiong, C. Pang, G. Li, and C. Hu, "Direct hydroxylation of benzene to phenol over TS-1 catalysts," *Catalysts*, vol. 8, no. 2, p. 49, 2018.
- [25] B. K. Kundu, V. Chhabra, N. Malviya, R. Ganguly, G. S. Mishra, and S. Mukhopadhyay, "Zeolite encapsulated host-guest Cu (II) Schiff base complexes: Superior activity towards oxidation reactions over homogenous catalytic systems," *Microporous Mesoporous Mater.*, vol. 271, pp. 100–117, 2018.
- [26] K. Akinlolu, B. Omolara, O. Kehinde, T. Shailendra, and M. Kumar, "Synthesis and characterization of Cu (II) and Co (II) encapsulated metal complexes in zeolite-Y for the oxidation of phenol and benzene," in *IOP Conference Series: Materials Science and Engineering*, 2019, vol. 509, p. 012061.
- [27] H. Liao *et al.*, "Benzene hydrogenation over polydopamine-modified MCM-41 supported Ruthenium-Lanthanum catalyst," *Inorg. Nano-Met. Chem.*, pp. 1–8, 2019.
- [28] M. Shahami, K. M. Dooley, and D. F. Shantz, "Steam-assisted crystallized Fe-ZSM-5 materials and their unprecedented activity in benzene hydroxylation to phenol using hydrogen peroxide," *J. Catal.*, vol. 368, pp. 354–364, 2018.
- [29] T. Ohtani, S. Nishiyama, and S. Tsuruya, "Liquid-phase benzene oxidation to phenol with molecular oxygen catalyzed by Cu-zeolites," *J. Catal.*, vol. 155, no. 1, 1995.
- [30] K. Rinramee, L. Sujarit, and S. Kornsanthia, " $\text{Fe}_2\text{O}_3$  on Zeolite NaY Synthesized from Rice Husk as Catalyst for Oxidation of Styrene," *RMUTP Res. J.*, vol. 13, no. 1, pp. 1–11, 2019.
- [31] S. Yamaguchi, A. Suzuki, M. Togawa, M. Nishibori, and H. Yahiro, "Selective Oxidation of Thioanisole with Hydrogen Peroxide using Copper Complexes Encapsulated in Zeolite: Formation of a Thermally Stable and Reactive Copper Hydroperoxo Species," *ACS Catal.*, vol. 8, no. 4, pp. 2645–2650, 2018.
- [32] Y. Huang, W. Wang, Q. Feng, and F. Dong, "Preparation of magnetic clinoptilolite/ $\text{CoFe}_2\text{O}_4$  composites for removal of  $\text{Sr}^{2+}$  from aqueous solutions: kinetic, equilibrium, and thermodynamic studies," *J. Saudi Chem. Soc.*, vol. 21, no. 1, pp. 58–66, 2017.
- [33] S. M. Montemayor, L. A. García-Cerda, and J. R. Torres-Lubián, "Preparation and characterization of cobalt ferrite by the

- polymerized complex method,” *Mater. Lett.*, vol. 59, no. 8–9, pp. 1056–1060, 2005.
- [34] N. Gill, A. L. Sharma, V. Gupta, M. Tomar, O. P. Pandey, and D. P. Singh, “Enhanced microwave absorption and suppressed reflection of polypyrrole-cobalt ferrite-graphene nanocomposite in X-band,” *J. Alloys Compd.*, vol. 797, pp. 1190–1197, 2019.
- [35] A. Wahab *et al.*, “Dye degradation property of cobalt and manganese doped iron oxide nanoparticles,” *Appl. Nanosci.*, pp. 1–10, 2019.
- [36] E. Manova *et al.*, “Mechano-synthesis, characterization, and magnetic properties of nanoparticles of cobalt ferrite,  $\text{CoFe}_2\text{O}_4$ ,” *Chem. Mater.*, vol. 16, no. 26, pp. 5689–5696, 2004.
- [37] X. Pan, L. Yan, C. Li, R. Qu, and Z. Wang, “Degradation of UV-filter benzophenone-3 in aqueous solution using persulfate catalyzed by cobalt ferrite,” *Chem. Eng. J.*, vol. 326, pp. 1197–1209, 2017.
- [38] E. Amini, K. Ahmadi, A. Rashidi, A. Youzbashi, and M. Rezaei, “Preparation of nanozeolite-based RFCC catalysts and evaluation of their catalytic performance in RFCC process,” *J. Taiwan Inst. Chem. Eng.*, vol. 100, pp. 37–46, 2019.
- [39] L. H. de Oliveira *et al.*, “ $\text{H}_2\text{S}$  adsorption on NaY zeolite,” *Microporous Mesoporous Mater.*, vol. 284, pp. 247–257, 2019.
- [40] E. Kianfar, “Nanozeolites: synthesized, properties, applications,” *J. Sol-Gel Sci. Technol.*, pp. 1–15, 2019.
- [41] A. S. Priya, D. Geetha, and N. Kavitha, “Effect of Al substitution on the structural, electric and impedance behavior of cobalt ferrite,” *Vacuum*, vol. 160, pp. 453–460, 2019.
- [42] I. O. Ali, “Sol–gel synthesis of  $\text{NiFe}_2\text{O}_4$  with PVA matrices and their catalytic activities for one-step hydroxylation of benzene into phenol,” *J. Therm. Anal. Calorim.*, vol. 116, no. 2, pp. 805–816, 2014.
- [43] I. Othman, R. M. Mohamed, I. A. Ibrahim, and M. M. Mohamed, “Synthesis and modification of ZSM-5 with manganese and lanthanum and their effects on decolorization of indigo carmine dye,” *Appl. Catal. Gen.*, vol. 299, pp. 95–102, 2006.

## الملخص العربي

محمد ثابت<sup>1,2</sup> و<sup>1</sup> ادهم الزمرراوي

<sup>1</sup> قسم الكيمياء ، كلية العلوم -جامعة الازهر - القاهرة

<sup>2</sup> قسم الكيمياء ، كلية العلوم ، جامعة جازان ، السعودية

تم تحضير فريت كوبلت  $\text{CoFe}_2\text{O}_4$  ، وتم دمجه و تحمليه على الزيوليت NaY بواسطة عملية الترسيب المشترك. كان التصميم الهيكلي للمركب  $\text{CoFe}_2\text{O}_4/\text{NaY}$  مميزاً من حيث النشاط والاستقرار. تم استخدام تقنيات مختلفة لوصف المحفزات مثل XRD ، FTIR ، وتحليل بنية المسام عن طريق امتزاز  $\text{N}_2$  عند 77 كلفن. ، و المورفولوجي SEM. ثبت أن  $\text{CoFe}_2\text{O}_4$  في العينة المركبة كان متفرقاً على سطح عينة الزيوليت، و يشير التشكل السطحي لـ SEM إلى أن  $\text{CoFe}_2\text{O}_4$  له بنية غير منتظمة من البلورات المجمعّة الكبيرة ، في حين أن  $\text{CoFe}_2\text{O}_4 / \text{NaY}$  أبدت في الغالب تشكلاً كروياً موحداً يشبه أحجام الجسيمات الصغيرة وتجويفات صغيرة على السطح الخارجي. تم فحص إضافة الهيدروكسيل إلى البنزين مع  $\text{H}_2\text{O}_2$  كعامل مؤكسد. كما تمت دراسة تأثير كمية  $\text{CoFe}_2\text{O}_4/\text{NaY}$  كمحفز، تركيز  $\text{H}_2\text{O}_2$  ، درجة الحرارة. أوضحت النتائج ، زيادة إنتاج الفينول بزيادة كميات  $\text{H}_2\text{O}_2$  ، والمحفز ، وزيادة درجة الحرارة. تم فحص حركية تفاعل الهيدروكسلة من البنزين إلى الفينول ، ومن البيانات، لوحظ أن كمية المحفز تؤثر بشدة على معدل التفاعل. تم تطبيق علاقة ارهينيوس لحساب طاقة التنشيط ، وكانت طاقة تنشيط المحفز 25.98 كيلو جول / مول.